

Thermally oxidized AlN thin films for device insulators

E. A. Chowdhury,^{a)} J. Kolodzey, J. O. Olowolafe, G. Qiu, G. Katulka, D. Hits, M. Dashiell, and D. van der Weide
Department of Electrical Engineering, University of Delaware, Newark, Delaware 19716

C. P. Swann and K. M. Unruh
Department of Physics and Astronomy, University of Delaware, Newark, Delaware 19716

(Received 4 February 1997; accepted for publication 19 March 1997)

The structural, optical, and electronic properties of an insulating material prepared by the thermal oxidation of AlN thin films on Si have been studied by a number of different experimental techniques. The thermal oxidation at 1100 °C of reactively sputtered AlN films on Si wafers was found to result in the formation of an oxide with a relative Al to O concentration near Al₂O₃ with small amounts of incorporated N. The structure of the AlO:N oxide could be varied between amorphous and polycrystalline, depending on the preparation conditions, and the oxide surface was found to be approximately three times smoother than the as-sputtered AlN films. Metal-oxide-silicon capacitors had an oxide charge density of about 10¹¹ cm⁻², capacitance-voltage characteristics similar to pure SiO₂, and a dielectric constant of 12.4. Infrared measurements yielded a refractive index of 3.9. These results indicate that thermally oxidized AlN films show promise as insulating structures for many integrated circuit applications, particularly for the case of III-V and group III-nitride based semiconductors. © 1997 American Institute of Physics. [S0003-6951(97)01920-7]

High quality insulating films are an essential component of many electronic devices. Insulating native oxides prepared by thermal oxidation are of particular importance because of the small defect densities characteristic of the buried interface, and the relative ease with which they can be formed. For example, thermally grown SiO₂ is routinely used as the gate insulator on Si based field-effect integrated circuits and as an insulating layer for interconnect wiring. Unfortunately, the native oxides of important III-V semiconductors [with the exception of AlAs (Refs. 1-3)] and group III nitrides (Refs. 4 and 5) have been unsuitable, either because they are unstable at circuit processing temperatures or are of insufficient quality. It is, therefore, of considerable technological importance to explore the possibility of preparing new insulating materials for integrated circuit applications. In this letter, we describe the preparation of such a material based on the thermal oxidation of AlN thin films to an AlO:N alloy with desirable optical and electronic properties.

To provide samples for oxidation, a series of AlN thin films was grown by reactive sputtering on *p*-type

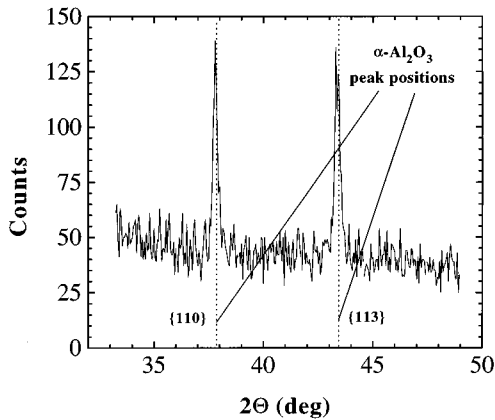


FIG. 2. X-ray diffraction spectrum of AlO:N oxide (sample No. 81705), with two peaks at 37.8°, and 43.3° in the 2θ diffraction angle, which correspond to the respective peaks of the (110) and (113) planes of α-Al₂O₃.

interface, which may or may not be desirable for optimum device properties. The use of substrates other than Si may also affect the oxide thickness. The RBS thickness error was estimated by curve fitting using RUMP software.⁶ Analysis suggested an upper limit of 7% for N in the AlO:N. The AES and EDAX compositions, calibrated using polycrystalline Al₂O₃ gauge standards, showed a 2:3 composition ratio for Al and O in the AlO:N layer, implying Al₂O₃ with a trace of N (<10%), in agreement with RBS. Most of the N from the AlN escaped during oxidation.

XRD measurements were performed at room temperature using a Phillips θ/2θ powder diffractometer with Cu Kα radiation. Some AlO:N films had broad, featureless x-ray spectra and were considered microcrystalline or amorphous, whereas some had peaks in the 30°–60° (2θ) range, as shown in Fig. 2, corresponding to tabulated values for α-Al₂O₃, and these films were considered polycrystalline. One AlO:N sample showed a broad, low intensity (202) peak at 2θ=45.76°, with grain diameter of ~3 nm estimated using Scherrer's formula,⁷ and another with different AlN deposition conditions had two x-ray diffraction peaks, as in Fig. 2, with ~40 nm grains. The AlO:N structure depended on the structure of the as-grown AlN films: microcrystalline AlN oxidized into amorphous AlO:N layers, and AlN having stronger XRD peaks oxidized into polycrystalline AlO:N.

Figure 3 shows an AFM scan of the AlO:N surface in air, performed using a Topometrix Explorer instrument. The rms roughness was ~1.2 nm, smaller than that of the as-grown AlN (rms ~4 nm). Oxidation caused distinct changes in the morphology: the as-grown AlN surface appeared granular, with grain diameters of ~68 nm; the oxidized surface appeared featureless, with small undulations perhaps caused by expansion of the surface with incorporation of O during oxidation.⁸

To assess the densities of the defect states and the charges in the composite AlO:N/SiO₂ oxide system, room-temperature capacitance versus voltage (C–V) measurements were performed at a frequency of 1 MHz using 329 μm diam Al metal contacts 300 nm thick. Figure 4 shows the C–V curve for an Al/oxide/Si structure having oxide sublayer thicknesses of 455 nm for the Al₂O₃ and 170 nm for the

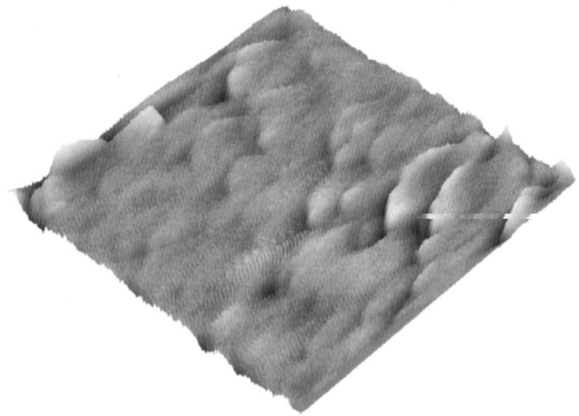


FIG. 3. AFM scan showing a birds-eye view of a 1000 nm×1000 nm surface region of AlO:N oxide (sample No. 90106), having a height range of 12.6 nm. The average height was 5.9 nm and the rms roughness was 1.2 nm.

SiO₂. At large negative voltages, the capacitance saturated, indicating accumulation. Near 0 V, the capacitance decreased, indicating depletion. Similar behavior had been previously observed by Schubert *et al.*³ with oxidized AlAs. To calculate the dielectric properties, the capacitance per unit area at the maximum (accumulation) C_{acc}, and the minimum (inversion) C_{inv}, were analyzed using the following equations:

$$C_{\text{acc}} = \frac{\epsilon_{\text{ox}}}{t_{\text{ox}}}, \quad C_{\text{inv}} = \left(\frac{t_{\text{ox}}}{\epsilon_{\text{ox}}} + \frac{W_{\text{dep}}}{\epsilon_s} \right)^{-1},$$

where $W_{\text{dep}} = (2\epsilon_s E_g / e^2 N_A)^{1/2}$ and ϵ_{ox} and ϵ_s are the electric permittivities of the oxide and the semiconductor, e is the magnitude of the electron charge, E_g is the band gap of Si, and $N_A = 5 \times 10^{15} \text{ cm}^{-3}$ is the Si substrate acceptor concentration (from four-point-probe resistivity measurements). For samples in which the total oxide layer comprised a bilayered structure of AlO:N and a thin layer of SiO₂ at the interface, we modeled the structure as two dielectrics in series. The sample of Fig. 4 having a total (combined AlO:N and

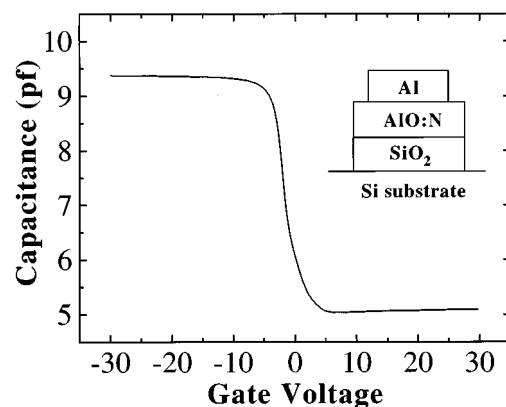


FIG. 4. Capacitance–voltage characteristic of Al/oxide/Si structure (sample No. 90106) with flatband voltage $V_{\text{FB}} = -2.723 \text{ V}$, threshold voltage $V_T = -0.783 \text{ V}$, oxide capacitance $C_{\text{acc}} = 9.38 \text{ pF}$, and insulator/depletion series capacitance $C_{\text{inv}} = 5.04 \text{ pF}$. Measurements were performed at room temperature at a frequency of 10⁶ Hz. The inset shows the layered structure used for measurements. The oxide layer comprised AlO:N and SiO₂ sublayers of thicknesses.

SiO₂) oxide thickness $t_{\text{ox}}=625$ nm (from RBS) and $\epsilon_{\text{ox}}=7.78\epsilon_0$ had $\epsilon_{\text{AlO:N}}=12.4\epsilon_0$ for the electric permittivity of the Al₂O₃, in agreement with tabulated values for α -Al₂O₃ (sapphire),⁹ where ϵ_0 is the permittivity of free space, and $\kappa=3.9$, was used for the dielectric constant of SiO₂.

The densities of fixed charge (Q_f) and interface trapped charge (Q_{it}) were combined into an effective defect charge density $Q_{\text{eff}}=(Q_f+Q_{\text{it}})$, for the total oxide comprising Al₂O₃ and SiO₂ sublayers, calculated from the shift in the metal–oxide–silicon flatband voltage (V_{FB}) according to¹⁰

$$V_{\text{FB}} = -\frac{Q_{\text{eff}}}{C_{\text{ox}}} + \Phi_{\text{ms}},$$

The total effective charge density for the sample of Fig. 4 was $(Q_{\text{eff}}/e)=+1.2\times 10^{11}\text{ cm}^{-2}$, where $\Phi_{\text{ms}}=-0.92$ V is the work function difference between the Al and Si. This Q_{eff} had contributions from both the AlO:N sublayer and the relatively thin SiO₂, which may have helped to reduce the net defect density. From Fig. 4, the flatband and the threshold voltages were near zero, indicating few defects and that the semiconductor Fermi level was not pinned at the oxide–semiconductor interface. These measurements demonstrated that the AlO:N/SiO₂ system possesses the charge control needed for insulated-gate field-effect transistor operation, with a higher dielectric constant than pure SiO₂. Fourier transform infrared (FTIR) measurements yielded a refractive index of 3.9 for the oxide at 1–2 μm wavelengths, in reasonable agreement with the C – V permittivity measurements.

We have shown that AlN thin films on Si can be thermally oxidized at 1100 °C producing the oxide Al₂O₃ with small quantities of N. The oxide structure varied from polycrystalline to amorphous, with a smooth surface. The high dielectric constant will permit more stored charge and thicker insulators than SiO₂ with its dielectric constant of

3.9. The capacitance–voltage characteristics demonstrated the control of the Si surface charge between accumulation and depletion, similar to the behavior of the conventional SiO₂/Si system. These results are encouraging for the possibility of novel compound semiconductor devices and circuits based on a new thermally oxidized nitride technology.

The authors are grateful to B. Orner for the FTIR measurements, Dr. P. R. Berger for ellipsometry measurements, M. Ahmed for the four-point-probe measurements, and Dr. J. Zavada and Lt. Col. Dr. G. Pomrenke for helpful discussions and encouragement. Special thanks to D. Smith for assistance with processing and measurements. This research was supported by DARPA Contract No. F49620-96-C-0006, and ARO Grant No. DAAH04-95-1-0625.

¹M. J. Ries, N. Holonyak, Jr., E. I. Chen, S. A. Maranowski, M. R. Islam, A. L. Holmes, and R. D. Dupuis, *Appl. Phys. Lett.* **67**, 1107 (1995).

²M. R. Krames, A. D. Minervini, and N. Holonyak, Jr., *Appl. Phys. Lett.* **67**, 73 (1995).

³E. F. Schubert, M. Passlack, M. Hong, J. Mannerts, R. L. Opila, L. N. Pfeiffer, K. W. West, C. G. Bethea, and G. J. Zydzik, *Appl. Phys. Lett.* **64**, 2976 (1994).

⁴R. J. Molner, R. Singh, and T. D. Moustakas, *Appl. Phys. Lett.* **66**, 268 (1995).

⁵A. Ozgur, W. Kim, Z. Fan, A. Botchkarev, A. Salvador, S.-N. Mohammad, B. Sverdlov, and H. Morkoc, *Electron. Lett.* **31**, 1389 (1995).

⁶L. R. Doolittle, *Nucl. Instrum. Methods Phys. Res. B* **9**, 344 (1985).

⁷B. D. Cullity, *Elements of X-ray Diffraction* (Addison-Wesley, New York, 1956).

⁸F. Ansart, H. Ganda, R. Saporte, and J. P. Traverse, *Thin Solid Films* **260**, 38 (1995).

⁹The dielectric constant of α -Al₂O₃ has components 11.5 and 9.65 parallel